JPEDAV (2004) 25:152-159
DOI: 10.1361/15477030418550
1547-7037/$19.00 ©ASM International

Evaluation of Phase Relations in the Nb-Cr-Al System at 1000 °C Using a Diffusion-Multiple Approach

J.-C. Zhao, M.R. Jackson, and L.A. Peluso

(Submitted 24 March 2003; in revised form 2 September 2003)

A high-efficiency diffusion-multiple approach was used to map most of the phase relations of the Nb-Cr-Al ternary system at 1000 °C. This system is very valuable for the design of niobium silicide-based composites. These composites have high potential as a replacement for Ni-base superalloys for jet engine applications. Both Cr and Al are alloying elements for these composites; thus the Nb-Cr-Al phase diagram, especially the stability of the oxidation-resistant Laves phase, is important information for the composite design. A partial 1000 °C isothermal section was constructed from the results obtained using electron probe microanalysis (EPMA) and electron backscatter diffraction (EBSD) from a diffusion multiple made up of Nb, Cr, $NbAl_3$, and $NbSi_2$. The stabilization of the C14 Laves phase by Al dominates the 1000 °C isothermal section, and the solubility of Al in the C14 Laves phase is as high as ~45 at.%.

1. Introduction

Niobium silicide-based composites show great promise for applications as the next generation turbine airfoil materials with significantly higher operating temperatures than those of current generation advanced Ni-base superalloys.[1-6] The Nb-Si binary composites have excellent creep strength, but poor oxidation resistance and poor room temperature fracture toughness.[1,2] Alloying with Cr and Al can improve the oxidation resistance. The potential application of these composites at very high temperatures requires a balance of high creep resistance, high oxidation resistance, and good low-temperature damage tolerance (fracture toughness). To achieve such a property balance, elements such as Cr, Ti, Hf, and Al are added to the composites, and significant progress has been made in improving the properties of the composites. Some of the alloying concepts were discussed by Zhao et al.[7] The advanced design of the composites requires a fair understanding of the phase equilibria in the Nb-Si-Ti-Cr-Hf-Al system. Since a reasonable definition of the Nb-Hf-Si system has been achieved,[8-10] our effort has been focused on the ternary systems Nb-Cr-Si, Nb-Si-Al, Nb-Cr-Al, Ti-Si-Cr, Ti-Si-Al, Ti-Cr-Al, Nb-Ti-Si, Nb-Ti-Cr, and Nb-Ti-Al. Other ternary systems related to the six-element system such as Nb-Ti-Hf, Nb-Cr-Hf, Nb-Hf-Al, Ti-Si-Hf, Ti-Cr-Hf, and Cr-Hf-Al have either good data or are less critical for the design of the Nb silicide composites. We report the results of the Nb-Cr-Al system in the present paper, and the results of other systems will be communicated separately.

In addition to being valuable for the design of the Nb silicide composites, the Nb-Cr-Al ternary phase diagram is also very useful for the design of other high-temperature alloys and coatings.[11-14] For instance, the Nb-rich aluminides, Nb_3Al and Nb_2Al, have demonstrated good strength and creep resistance at high temperatures.[11,12] The Al-rich intermetallic phase $NbAl_3$ is also a candidate material for advanced aeropropulsion systems due to its high melting point and low density. Cr addition is very important for the oxidation resistance of these aluminides and coatings.

The high-efficiency "diffusion multiple" approach[15-18] is ideally suited for mapping phase diagrams of the six-element related systems mentioned earlier. It would take hundreds of alloys to determine the nine ternary systems using the traditional one-alloy-at-a-time (equilibrated alloy) approach. For instance, it took Goldschmidt and Brand[19] about 220 alloys to map just the Nb-Cr-Si ternary system and similarly about 135 alloys were used by Lysenko et al.[20] to determine the Ti-Cr-Si system. These alloys have very high melting temperatures and are difficult to make and to homogenize. Extra effort also needs to be taken to avoid interstitial (oxygen, nitrogen, carbon, etc.) contamination during alloy casting and heat treatment. In contrast, the diffusion multiple approach needs only a few cast alloys, and the samples were easy to make. Safeguarding against the interstitial contamination can be very easily implemented, as will be discussed later. The general diffusion-multiple approach was discussed in detail previously[15-18] and has been successfully applied to many alloy systems.

The constitutive binary phase diagrams of the Nb-Cr-Al system, i.e., Nb-Al,[21] Nb-Cr,[22,23] and Al-Cr[24-29] are already available in the literature. There is still active research on the phase diagram of the Al-Cr binary system.[26,27] The crystal structures of the phases in the binary and the ternary system are listed in Table 1.[27,30-33]

The first isothermal section of the Nb-Cr-Al systems was reported by Hunt and Raman[34] for 1000 °C, as shown in Fig. 1(a). It provided a rough overview of this system, but most of the phase boundaries and the tie-triangles were undefined. Mahdouk and Gachon[35] recently reported an isothermal section at 1000 °C (Fig. 1b) based on electron probe microanalysis (EPMA) of small-charge samples pro-

---

J.-C. Zhao, M.R. Jackson, and **L.A. Peluso,** General Electric Company, GE Global Research Center, P.O. Box 8, Schenectady, NY 12301. Contact e-mail: zhaojc@research.ge.com.

duced in a direct reaction calorimeter and then annealed at 1000 °C for 168 h (1 week). There are large discrepancies with regard to Cr solubility in Nb aluminides ($NbAl_3$, Nb_2Al, and Nb_3Al) and body-centered-cubic (bcc) (Nb) between the results of Mahdouk and Gachon[35] and Hunt and Raman.[34] In addition, the phase equilibria between the two $Nb(Cr,Al)_2$ Laves phases, *C*15 and C14, are not determined. Our work will help in comparing and judging the reliability of the literature data and generating new data for the phase equilibria of the Nb-Cr-Al ternary system.

2. Experimental Method

A diffusion multiple with the cross-section view shown schematically in Fig. 2(a) was made. The dimensions were designed so that the pieces of pure elements and compounds are much larger than the diffusion distance; thus there will be pure elements and compounds left after the long-term diffusion annealing. To avoid the low melting point of Al, we used both $NbAl_3$ and $NbSi_2$ compounds as members of the diffusion multiple. Both these compounds were made

Table 1 Crystal Structure of Phases in the Nb-Cr-Al Ternary System; the Data Were Taken From Villars and Calvert[30] for Most Phases, From Knapp[31] for Cr_4Al_9, Ellner et al.[32,33] for Cr_4Al_8, and From Audier, et al.[27] for $CrAl_4$ and Cr_2Al_{11}.

			Lattice Parameter, nm			
Phase	**Pearson Symbol**	**Space Group**	***a***	***b***	***c***	**γ**
Al	*cF*4	$Fm\bar{3}m$	0.40497			
Cr	*cI*2	$Im\bar{3}m$	0.28847			
Nb	*cI*2	$Im\bar{3}m$	0.33067			
Cr_2Al	*tI*6	*I*4/*mmm*	0.3005		0.8649	
Cr_5Al_8	*hR*26	$R\bar{3}m$	1.2813		0.7951	120°
Cr_4Al_9	*cI*52	$I\bar{4}3m$	0.9123			
$CrAl_4$	*hP*574	$P6_3/mmc$	1.998		2.467	119.33°
Cr_2Al_{11}	*oC*16	*Cmcm*	1.24	3.46	2.02	122.20°
$CrAl_7$	*mC*104	*C*2/*m*	2.5256	0.7582	1.0955	128.68°
Nb_2Al	*tP*30	$P4_2/mmm$	0.9945		0.5171	
Nb_3Al	*cP*8	$Pm\bar{3}n$	0.5186			
$NbAl_3$	*tI*8	*I*4/*mmm*	0.3844		0.8605	
$NbCr_2$-C14 Laves	*hP*12	$P6_3/mmc$	0.4931		0.8123	120°
$NbCr_2$-C15 Laves	*cF*24	$Fd\bar{3}m$	0.695			

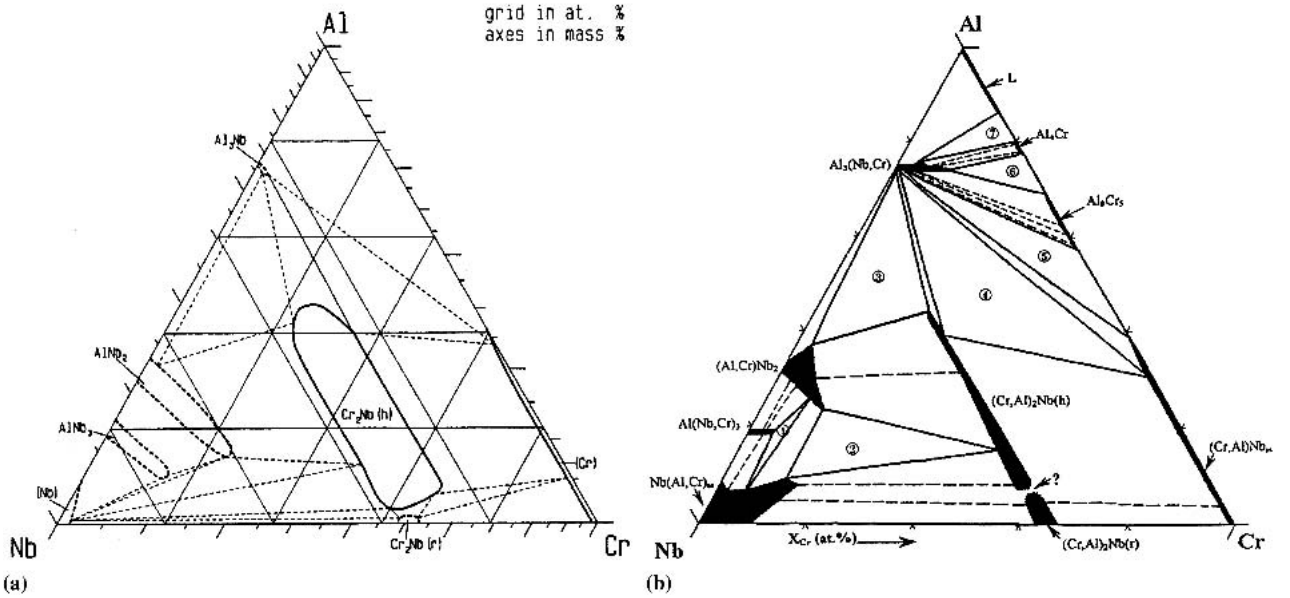

Fig. 1 The 1000 °C isothermal sections of the Nb-Cr-Al ternary system from the literature: **(a)** an approximate phase diagram reported by Hunt and Raman[34] showing that phase boundaries and tie-triangles were not well defined; and **(b)** an isothermal section recently reported by Mahdouk and Gachon.[35]. Tie-lines are indicated by dashed lines. The question mark indicates that the limits of the two forms of $Nb(Cr,Al)_2$ Laves phases are not determined accurately.

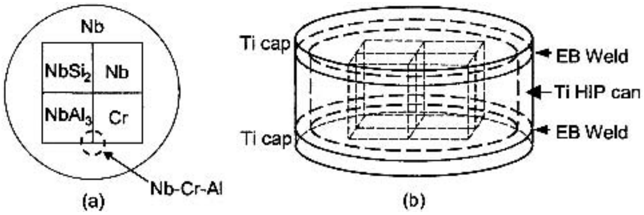

Fig. 2 A diffusion multiple for efficient mapping of the Nb-Cr-Al ternary phase diagram: **(a)** cross-sectional view; and **(b)** perspective view. See text for the size of the sample. The results reported in this work were all obtained from the tri-junction corner of Nb-Cr-NbAl$_3$ circled in (a).

using arc melting. They were then cut into square bars of 7 × 7 × 25 mm using electro-discharge machining (EDM). A 14 × 14 mm square opening was cut from a 25 mm diameter × 25 mm height cylindrical piece of pure Nb. The square opening was cut across the whole height of the Nb piece. Pieces of high-purity Nb and Cr in the dimension of 7 × 7 × 25 mm were also machined using EDM. The re-cast layer on the EDMed surfaces was removed by mechanical grinding to make clean surfaces. The pieces were ultrasonically cleaned in methanol and then assembled into the geometry shown in Fig. 2(a). The height of all pieces was 25 mm. The assembled diffusion multiple was then loaded into a hot isostatic press (HIP) can made of commercial purity Ti, which is schematically shown in Fig. 2(b). A 25 μm layer of Ta was placed between the diffusion multiple and the HIP can to isolate any interstitial contaminants that may diffuse into the HIP can from the quartz capsule during long-term annealing. The top and bottom caps of the HIP can were electron beam welded. HIPing was performed at 1200 °C, 200 MPa for 4 h. The HIP can containing the diffusion multiple was then encapsulated in an evacuated quartz tube backfilled with pure argon. Since Nb is susceptible to oxygen and nitrogen contamination, it is critical to keep the diffusion multiple free from interstitial elements. To further absorb any oxygen that may diffuse into the quartz tube, a packet of pure yttrium was wrapped in Ta foils and was then placed inside the quartz tube. Thus, the diffusion multiple was protected from the intersitials (O, N, C, etc.) by the quartz tube, the pure yttrium absorber, the Ti HIP can, and the Ta diffusion barrier. The encapsulated sample was then annealed at 1000 °C for 2000 h. After the heat treatment, the quartz capsule containing the diffusion multiple was taken from the Ar furnace and cooled down to ambient temperature by breaking the quartz tube and quenching the diffusion multiple into water. The diffusion multiple was cut into halves parallel to the ends using wire EDM, and then ground and polished.

The samples were first examined using scanning electron microscopy (SEM), especially the backscattered electron (BSE) imaging. Most phases could be seen (although not identified explicitly) in the BSE images due to the differences in their average atomic weight. Quantitative EPMA analysis was performed on a CAMECA SX50 (Paris, France) microprobe equipped with four wavelength dispersion spectrometers (WDS) at a 40° take-off angle. The electron beam condition used for EPMA analysis was at 15 keV, 30 nano-amperes focused to a small spot (x-ray excitation volume approximately 1 cubic micron). Pure elemental standards were used for all elements calibrated: Nb L_α, Cr K_α, and Al K_α, and beam current was varied to 5 nanoamperes for Al in calibrations to avoid saturation of the detector in their respective gas flow proportional counters. The Nb L_α analysis was performed using a Pentaerythritol (PET) crystal with a $2d$ spacing of 8.74 Å. Al K_α x-ray measurements were done using thallium acid phthalate (TAP) crystals with a $2d$ spacing of 25.75 Å, and Cr K_α was measured using a lithium fluoride (LiF) crystal, with a $2d$ spacing of 4.027 Å. Data reduction (from x-ray intensity ratios to composition in weight percent) was performed using a modified $\phi\rho z$ program inherent to the CAMECA microprobe.

Electron backscatter diffraction (EBSD) analysis was performed to obtain crystal structure information of the phases formed in the diffusion multiple. Phase identification was accomplished by a direct match of the diffraction bands in the experimental backscatter pattern with simulated patterns generated using known structure types and lattice parameters. A detailed discussion on this powerful EBSD technique can be found in Schwartz et al.[36]

3. Results and Discussion

Backscattered electron images taken from the Nb-Cr-NbAl$_3$ tri-junction (schematically circled area in Fig. 2a) of the diffusion multiple annealed at 1000 °C for 2000 h are shown in Fig. 3. During the long-term diffusion treatment, extensive interdiffusion among Nb, Cr, and Al took place, and all the equilibrium phases, including the intermetallic phases, formed by interdiffusion reactions. The black area on top of Fig. 3(a) was a crack probably formed during specimen preparation (EDM cutting, grinding, and polishing). The Nb$_2$Al and Nb$_3$Al phases, which are difficult to see in Fig. 3(a), can be seen in Fig. 3(b) and (c). Even in Fig. 3(b), the Nb$_3$Al is still difficult to see since the atomic number contrast among Nb$_2$Al, Nb$_3$Al, and bcc (Nb) is very low. At the location of Fig. 3(b), Nb$_3$Al started to disappear (thus it is very thin in this area); i.e., it was de-stabilized by Cr on the right-hand side of the image where higher Cr concentration was present. Figure 3(c) is at the location where Nb$_2$Al started to disappear; i.e., this phase was also destabilized by Cr on the right-hand side of the image where higher Cr concentration was present. Note that at the locations of Fig. 3(b) and (c), as the Nb$_3$Al and Nb$_2$Al phases were extremely thin, we took into account of overlapping and over-sampling effects when analyzing the EPMA data.

EBSD was used to identify the phases, especially the two different types of Laves phases, the hexagonal C14 and the cubic C15. A backscattered electron image alone cannot differentiate them since their compositions in equilibrium are very close to each other, thus having very similar average atomic number density. The phase interface between C14 and C15 was identified using EBSD and was shown in Fig. 3(c) with a dashed line. This was accomplished by moving the electron beam around in the Laves phase regions and taking EBSD patterns manually. The EBSD pattern from C15 was relatively faint and difficult to analyze

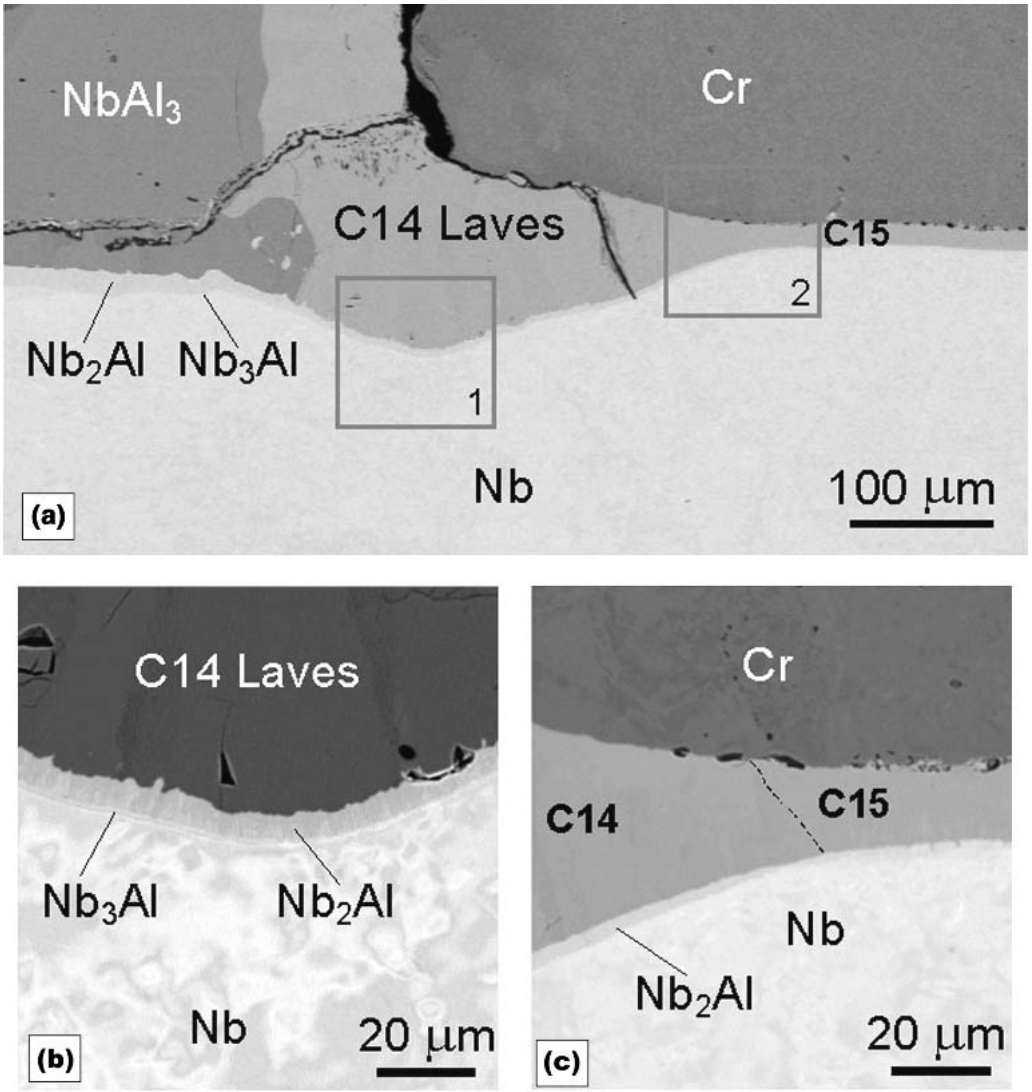

Fig. 3 Backscattered electron SEM images of the Nb-Cr-$NbAl_3$ tri-junction area of the diffusion multiple (Fig. 2) annealed at 1000 °C for 2000 h showing the formation of many different intermetallic compounds: **(a)** a low-magnification image showing the overall tri-junction and locations 1 and 2, **(b)** a high-magnification image of location 1 showing the very thin layers of Nb_2Al and Nb_3Al, and **(c)** a high-magnification image of location 2 showing the location of the Nb_2Al phase and the location of the C14 Laves to C15 Laves transition (dashed line).

using automated EBSD pattern collection and indexing mode. The EBSD patterns of the C14 and C15 Laves phases are shown in Fig. 4. Identification of the interface between C14 and C15 allowed us to determine two three-phase equilibria [C14+C15+bcc(Nb) and C14+15+bcc(Cr)] very accurately. We clearly defined, for the first time, these two three-phase regions.

EBSD was also used to identify the Nb aluminide phases, Nb_3Al, Nb_2Al, and $NbAl_3$. Since the Nb_3Al phase was very thin, its EBSD pattern is relatively faint, but clearly indexable (Fig. 5a). Typical EBSD patterns of the Nb aluminide phases collected from the diffusion multiple are shown in Fig. 5.

By performing EPMA analysis in the Nb-Cr-$NbAl_3$ tri-junction area, a large amount of phase equilibrium information was obtained. Based on the compositional information from EPMA and by taking advantage of the local equilibrium at phase interfaces, a partial isothermal section of the Nb-Cr-Al system for 1000 °C was constructed as shown in Fig. 6. Detailed procedures for phase diagram mapping using diffusion multiples can be found elsewhere.[15-18]

The new 1000 °C isothermal section of the Nb-Al-Cr ternary system shows the same phase relationships as those reported by Hunt and Raman[34] as well as by Mahdouk and Gachon.[35] Due to the fact that we used $NbAl_3$ instead of pure Al as a member of the diffusion multiple, we did not obtain any phase equilibrium information at the Al-rich end of the phase diagram. This is also partly due to the very stable nature of the C14 Laves phase, which dominates the center of the phase diagram. Nevertheless, we still obtained a large amount of information for seven single-phase regions and five three-phase regions. Identical to the obser-

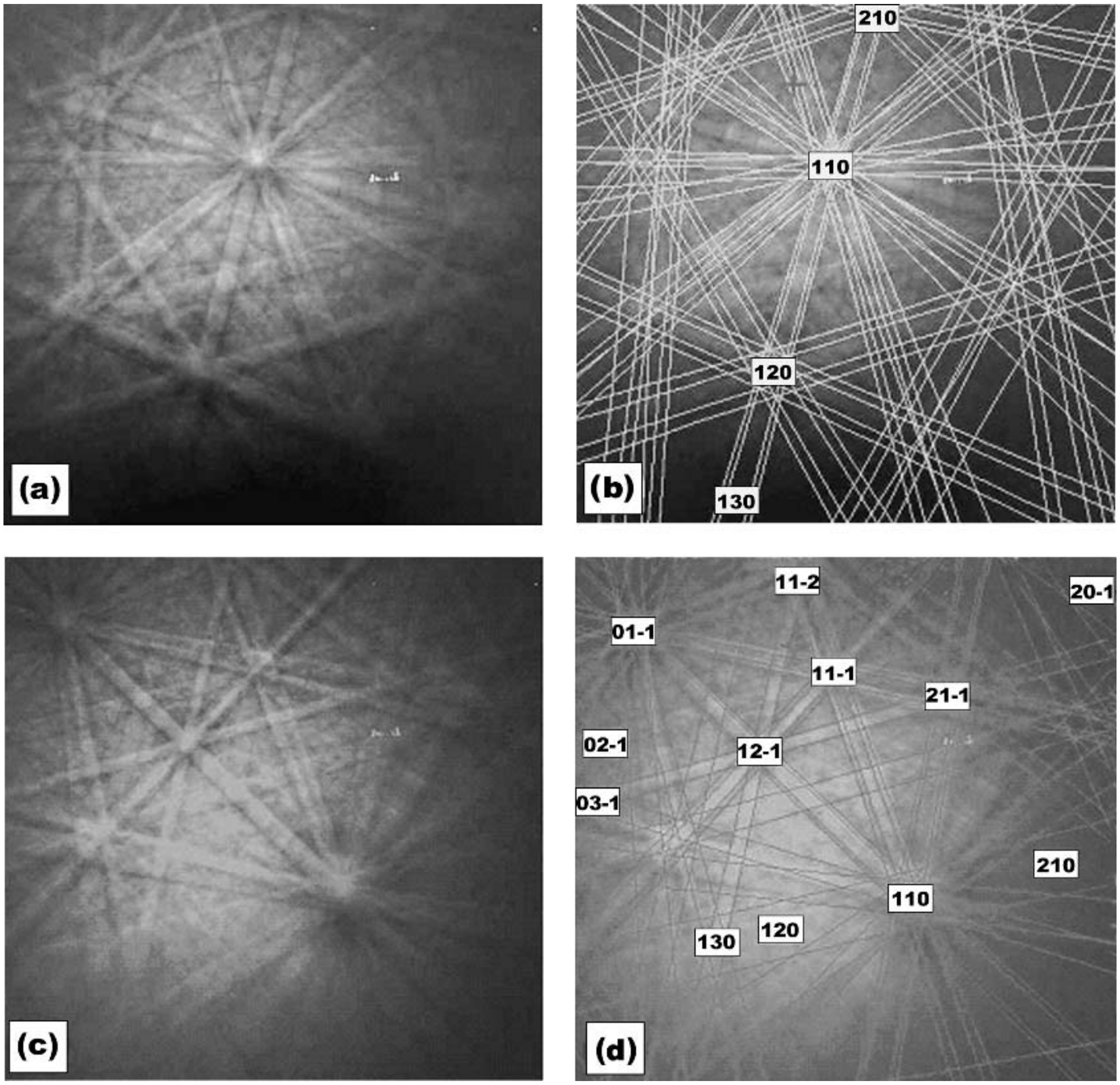

Fig. 4 EBSD patterns of the Laves phases formed in the Nb-Cr-$NbAl_3$ tri-junction area of the diffusion multiple (Fig. 2) annealed at 1000 °C for 2000 h: **(a)** and **(b)** C14 Laves, and **(c)** and **(d)** C15 Laves. The un-indexed patterns are shown on the left and the indexed patterns on the right.

vations of Hunt and Raman[34] as well as those of Mahdouk and Gachon,[35] the stabilization of the high-temperature hexagonal C14-Laves phase of the binary Cr-Nb system ($NbCr_2$) by Al addition was observed, and the solubility of Al in C14 was as high as ~45 at.%, which is consistent with previous observations.[34,35] The composition of the C14 Laves phase was almost a line-compound in the form of $Nb(Cr,Al)_2$. Our result is consistent with that of Mahdouk and Gachon,[35] and the results together suggest that the very wide (Nb variation) phase region of the C14 Laves reported by Hunt and Raman[34] is unrealistic. The widening of the C14 Laves phase region in the case of Hunt and Raman[34] was probably due to segregation during primary solidification of C14-Laves. The C14 Laves with composition away from $Nb(Cr,Al)_2$ formed during solidification did not have sufficient time to decompose due to its sluggish kinetics. In our diffusion multiple, the C14 Laves formed at 1000 °C by diffusion reactions and it did not go through the solidification process; thus it is much easier to reach local equilibrium at the phase interfaces. In the case of Mahdouk and Gachon,[35] the direct reaction calorimetry process involves fine powders that react together in the solid state; thus it also avoids the problem associated with melting and solidification. The work of both Hunt and Raman[34] and Mahdouk and Gachon[35] is a great example to show that it is much easier to reach equilibrium by solid-state reactions than to go through a solidification and decomposition process when involving high-melting compounds whose decomposition kinetics are sluggish. Both Hunt and Raman[34] and Mahdouk and Gachon[35] annealed their samples at 1000 °C for 168 h (1 week); Mahdouk and Gachon reached equilibrium through solid-state reactions, whereas Hunt and Raman did not reach equilibrium for the C14 Laves using melting/solidification and decomposition annealing.

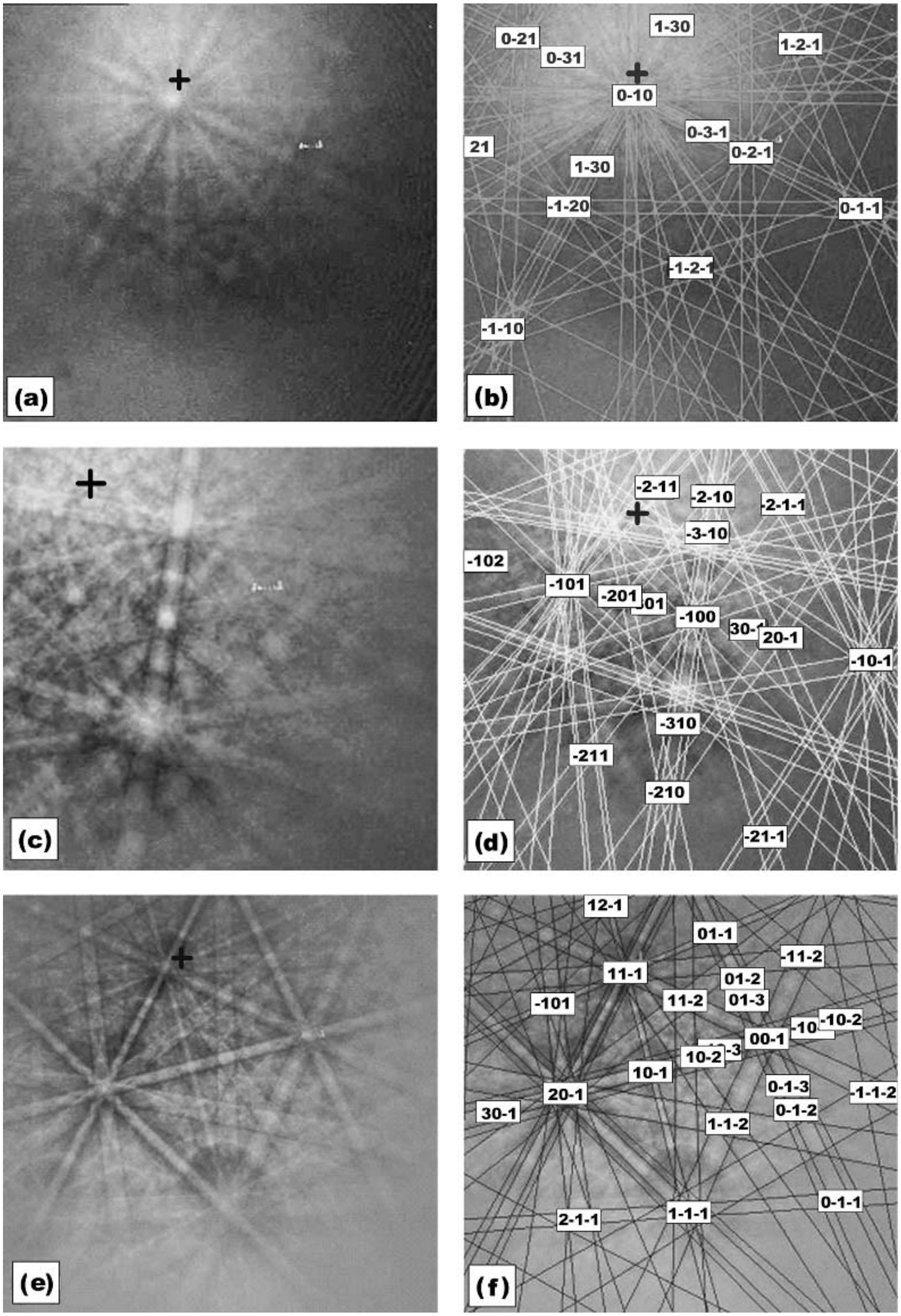

Fig. 5 EBSD patterns of Nb aluminide phases formed in the Nb-Cr-$NbAl_3$ tri-junction area of the diffusion multiple (Fig. 2) annealed at 1000 °C for 2000 h: **(a)** and **(b)** Nb_3Al; **(c)** and **(d)** Nb_2Al; and **(e)** and **(f)** $NbAl_3$. The un-indexed patterns are shown on the left and the indexed patterns on the right.

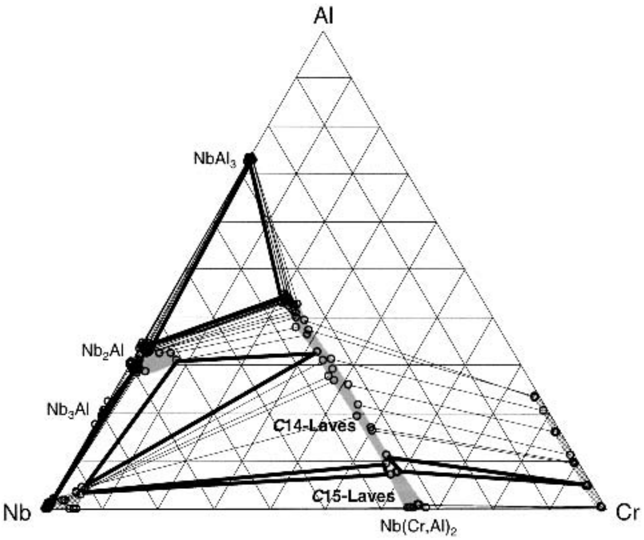

Fig. 6 The 1000 °C partial isothermal section of the Nb-Cr-Al system obtained from the Nb-Cr-NbAl$_3$ tri-junction area of the diffusion multiple annealed at 1000 °C for 2000 h. The phase diagram is plotted in atomic percent axes with the numbers removed for simplicity. The solid triangles indicate well-defined three-phase equilibria and the open circles show the tie-line compositions. The tie lines are shown with thin lines.

Most of the results obtained from the diffusion multiples agreed well with those reported by Mahdouk and Gachon[35] except the bcc (Nb) + C14 Laves + Nb$_2$(Al,Cr) three-phase equilibrium. Our result showed much higher Al concentration in the C14 Laves phase in equilibrium with both bcc (Nb) and Nb$_2$(Al,Cr). Several tie-lines in the bcc (Nb) + C14 two-phase region and in the Nb$_2$Al + C14 two-phase region clearly show the trend of high Al (>20 at.%) concentration in the C14 Laves phase in equilibrium with bcc(Nb) and Nb$_2$Al. In addition, we observed very low solubility of Cr in Nb$_3$Al, which is slightly different from the result of Mahdouk and Gachon[35] (Fig. 1b). The limited thickness of the Nb$_3$Al and Nb$_2$Al phases, especially the Nb$_3$Al phase, may have introduced some error in the EPMA data obtained from the diffusion multiple and may have contributed to the some of the difference in results between this study and that of Mahdouk and Gachon, even though we have taken into account the overlapping and oversampling effect during EPMA data analysis.

In Nb silicide composites with both Cr and Al additions, both elements help promote the C14-Laves phase (instead of the *A*15 Nb$_3$Al phase for the Al case). The alloying effect of Cr and Al in Nb silicide-based composites can be appreciated by examining the Nb-Cr-Si, Nb-Al-Si and Nb-Cr-Al phase diagrams. Our work on the Nb-Cr-Si and Nb-Al-Si ternary systems were reported separately.[36,37]

The phase equilibrium information of the Nb-Cr-Al system is very useful for the design of both Nb silicide composites and coatings for these composites. This is one of the key systems recommended for CALPHAD modeling to add data to the developing thermodynamic database for Nb silicide-based systems.[10,39,40]

4. Conclusions

Using the high-efficiency diffusion-multiple approach, we mapped part of the 1000 °C isothermal section of the Nb-Cr-Al ternary system. There was no ternary compound in this ternary system. The high-temperature C14 Laves of the Cr-Nb binary system was stabilized to 1000 °C by Al addition, and the Al solubility in the C14 Laves is as high as ~45 at.%. We reported results on seven single-phase regions and five three-phase regions. Our results are in good agreement with the data reported by Hunt and Raman[34] as well as Mahdouk and Gachon[35] in terms of the expected phase relations.

Acknowledgments

The authors are grateful to A.M. Ritter and B.P. Bewlay for support and/or valuable discussions. We are also thankful for Lizhen Tan for his help in preparing the manuscript and L.N. Brewer for EBSD analysis. This work was supported by the U.S. Air Force Office of Scientific Research (AFOSR) under grant number F49620-99-C-0026 with C. Hartley as a program manager. The views and conclusions contained herein are those of the authors and should not be interpreted as necessarily representing the official policies or endorsement, either expressed or implied, of the AFOSR or the U.S. Government.

References

1. M.G. Mendiratta and D.M. Dimiduk: "Microstructures and Mechanical Behavior of Two-Phase Niobium Silicide-Niobium Alloys," *Mater. Res. Soc. Symp. Proc.*, 1989, *133,* pp. 441-46.
2. M.R. Jackson, B.P. Bewlay, R.G. Rowe, D.W. Skelly, and H.A. Lipsitt: "High-Temperature Refractory Metal-Intermetallic Composites," *JOM*, 1996, *48,* pp. 39-44.
3. P.R. Subramanian, M.G. Mendiratta, and D.M. Dimiduk: "The Development of Nb-Based Advanced Intermetallic Alloys for Structural Applications," *JOM*, 1996, *48,* pp. 33-38.
4. B.P. Bewlay, J.J. Lewandowski, and M.R. Jackson: "Refractory Metal-Intermetallic In-Situ Composites for Aircraft Engines," 1997, *49,* pp. 44-45.
5. S.J. Balsone, B.P. Bewlay, M.R. Jackson, P.R. Subramanian, J-C. Zhao, A. Chatterjee, and T. Heffernan, "Materials Beyond Superalloys—Exploiting High-Temperature Composites" in *Structural Intermetallics 2001*, K. Hemker, D.M. Dimiduk, H. Clemens, R. Darolia, H. Inui, J.M. Larsen, V.K. Sikka, M. Thomas, and J.D. Whittenberger, ed., TMS, Warrendale, PA, 2001, pp. 99-108.
6. B.P. Bewlay, M.R. Jackson, J.-C. Zhao, and P.R. Subramanian: "A Review of Very High-Temperature Nb-Silicide Composites," *Metall. Mater. Trans.,* in press.
7. J-C. Zhao, B.P. Bewlay, M.R. Jackson, and L.A. Peluso: "Alloying and Phase Stability in Niobium Silicide In-Situ Composites" in *Structural Intermetallics 2001,* K. Hemker, D.M. Dimiduk, H. Clemens, R. Darolia, H. Inui, J.M. Larsen, V.K. Sikka, M. Thomas, and J.D. Whittenberger, ed., TMS, Warrendale, PA, 2001, pp. 483-91.
8. B.P. Bewlay, R.R. Bishop, and M.R. Jackson: "The Nb-Hg-Si Ternary Phase Diagram: Liquid-Solid Phase Equilibria in Nb- and Hf-Rich Alloys," *Z. Metallkde*., 1999, *90,* pp. 413-22.
9. J-C. Zhao, B.P. Bewlay, and M.R. Jackson: "Determination of Nb-Hf-Si Phase Equilibria," *Intermetallics,* 2001, *9,* pp. 681-89.

10. Y. Yang, Y.A. Chang, J-C. Zhao, and B.P. Bewlay: "Thermodynamic Modeling of the Nb-Hf-Si Ternary System," *Intermetallics,* 2003, *11,* 407-15.
11. D.L. Anton and D.M. Shah: "Prospects, Promises and Properties of Refractory Intermetallics," *Mater. Res. Soc. Symp. Proc.*, 1993, *288,* pp. 141-50.
12. D.M. Dimiduk, P.R. Subramanian, and M.G. Mendiratta: "Exploration of Niobium-Based Advanced Intermetallics Materials," *Acta Metall. Mater.*, 1995, *8,* pp. 519-30.
13. M.G. Hebsur, J.R. Stephens, J.L. Smialek, C.A. Barrett, and D.S. Fox: "Influence of Alloying Elements on the Oxidation Behavior of $NbAl_3$," *Sci. Tech. Aerosp. Rep.*, 274 1989 Abstr. No. N89-12717.
14. J. Doychak and M.G. Hebsur: "Protective Al_2O_3 Scale Formation on $NbAl_3$-Base Alloys," *Oxid. Met.*, 1991, *36,* p. 113.
15. J-C. Zhao: "A Combinatorial Approach for Structural Materials," *Adv. Eng. Mater.*, 2001, *3,* pp. 143-47.
16. J-C. Zhao: "A Combinatorial Approach for Efficient Mapping of Phase Diagrams and Properties," *J. Mater. Res.*, 2001, *16,* pp. 1565-78.
17. J-C. Zhao, M.R. Jackson, L.A. Peluso, and L. Brewer: "A Diffusion Multiple Approach for Accelerated Design of Structural Materials," *MRS Bull.*, 2002, *27,* pp. 324-29.
18. J-C. Zhao, M.R. Jackson, L.A. Peluso, and L. Brewer: "A Diffusion-Multiple Approach for Mapping of Phase Diagrams, Hardness, and Elastic Modulus," *JOM*, 2002, *54*(7), pp. 42-45.
19. H.J. Goldschmidt and J.A. Brand: "The Constitution of the Chromium-Niobium-Silicon System," *J. Less-Common Met.*, 1961, *3,* pp. 34-43.
20. L.A. Lysenko, V.Ya. Markiv, O.V. Tsybukh, and E.I. Gladyshevskii: "Ti-Cr-Si System," *Inorganic Mater.,* 1971, *71,* pp. 157-59.
21. U.R. Kattner: "Al-Nb (Aluminum-Niobium)" in *Binary Alloy Phase Diagrams*, 2nd ed., T.B. Massalski, ed., ASM International, Materials Park, OH, 1990.
22. M. Venkatraman and J.P. Neumann: "Cr-Nb (Chromium-Niobium)" in *Binary Alloy Phase Diagrams*, 2nd ed., T.B. Massalski, ed., ASM International, Materials Park, OH, 1990.
23. J.G.C. Neto, S.G. Fries, and H.L. Lukas: "Thermodynamic Optimisation of the Nb-Cr System," *CALPHAD*, 1993, *17,* pp. 219-28.
24. J.L. Murray: "Al-Cr (Aluminum-Chromium)" in *Binary Alloy Phase Diagrams*, 2nd ed., T.B. Massalski, ed., ASM International, Materials Park, OH, 1990.
25. J.G.C. Neto, S. Gama, and C.A. Ribeiro: "Experimental Study of the Al—Cr Equilibrium Diagrams," *J. Alloys Compd.*, 1992, *182,* pp. 271-80.
26. K. Mahdouk and J.C. Gachon: "Thermodynamic Investigation of the Aluminum-Chromium System," *J. Phase Equili.,* 2000, *21,* pp. 157-66.
27. K. Mahdouk, J.C. Gachon: "New Results About the Al-Cr Binary Phase Diagram," *Arch Metal.*, 2001, *46,* pp. 233-38.
28. M. Audier, M. Durandcharre, E. Laclau, H. Klein: "Phase Equilibria in the Al-Cr System," *J. Alloys Compounds,* 1995, *220,* pp. 225-30.
29. X.Z. Li, K. Sugiyama, K. Hiraga, A. Sato, A. Yamamoto, H.X. Sui, and K.H. Kuo: "On the Structure of the Al_4Cr Epsilon Phase and Its Relation to the Al-Cr-Ni Kappa Phase," *Z. Kristallographie*, 1997, *212,* pp. 628-33.
30. P. Villars and L.D. Calvert: *Pearson's Handbook of Crystallographic Data for Intermetallic Phases*, 2nd ed., ASM International, Materials Park, OH, 1991.
31. A. Knapp: "Magnetische Untersuchungen in Dreistoffsystem Aluminium-Chrom-Kupfer," *Z. Metallkd.*, 1941, *33,* pp. 153.
32. M. Ellner, J. Braun, and B. Predel: "X-Ray Investigations on the Cr—Al Phases Belonging to the Tungsten Family," *Z. Metallkd.*, 1989, *80,* pp. 374-83.
33. J. Braun, M. Ellner, and B. Predel: "Structure of the High-Temperature Phase Cr_5Al_8 (h)," *J. Alloys Comps.*, 1992, *183,* pp. 444-48.
34. C.R. Hunt and A. Raman: "Alloy Chemistry of $\sigma(\beta U)$-Related Phases," *Z. Metallkd.*, 1968, *59,* pp. 701-707.
35. K. Mahdouk and J.C. Gachon: "A Thermodynamic Study of the Al-Cr-Nb Ternary System," *J. Alloys Compd.*, 2001, *321,* pp. 232-36.
36. Anon., *Electron Backscatter Diffraction in Materials Science,* A.J. Schwartz, M. Kumar, and B.L. Adams, ed., Kluwer Academic / Plenum Publishers, New York, 2000.
37. J-C. Zhao, M.R. Jackson, and L.A. Peluso: "Determination of the Nb-Cr-Si Phase Diagram Using Diffusion Multiples," *Acta Mater.*, 2003, *51,* 6395–405.
38. J-C. Zhao, M.R. Jackson, and L.A. Peluso: "Phase Diagram of the Nb-Al-Si Ternary System," *J. Alloys Compd.*, 2003, *360,* pp 183–88.
39. H. Liang and Y.A.Chang, "Thermodynamic Modeling of the Nb-Si-Ti Ternary System," *Intermetallics*, 1999, *7,* pp. 561.
40. Y. Yang and Y.A. Chang: University of Wisconsin – Madison, private communication, 2002.